First International Conference on
Bio-based Building Materials

June 22nd - 24th 2015
Clermont-Ferrand, France

STUDY OF LIME AND HEMP CONCRETE (LHC) – MIX DESIGN, CASTING PROCESS AND MECHANICAL BEHAVIORS

T. Lecompte*, P. Tronet, V. Picandet, C. Baley
Université de Bretagne Sud, EA4250, LIMATB F, 56100 Lorient, France
*Corresponding author; e-mail address: thibaut.lecompte@univ-ubs.fr

Abstract
This paper deals with the mechanical behavior of lime and hemp composites. LHC blocks have been processed by compression in a rigid die at a relatively high compression pressure. It allows producing LHC with a high proportion of hemp shiv. New mechanical parameters are proposed to compare experimental results of this study with those of literature. This paper shows that a high pressure of compaction enhances the compressive strength, and can offset a lack of binder. Consequently, a new formula is proposed to predict the strength of LHC, depending on both the binder content and the compaction state of the shiv particles. It leads to some recommendations for the mix design of such composites

Keywords:
Lime and hemp composite, mix design, compression moulding, rigid die, compressive strength, compressive stiffness

1 INTRODUCTION

Nowadays the most developed bio-aggregate-based building material in Europe is LHC: lime and hemp composite. This material associates a mineral binder, often a combination of hydraulic and non-hydraulic lime, with a plant-based aggregate, mostly consisting in shiv, without or with little residual fibers. Shiv is produced from the woody core of hemp stem, grounded and sieved into 5 to 40mm-in-length particles [Picandet 2013]. Due to the environmental assets of non-hydraulic lime and of hemp growing, LHC presents, during its life cycle, a weaker ecological impact [Arnaud 2000, Boutin 2006] compared to traditional building materials. However, LHC has properties that differ from those of conventional concrete. It is lighter, with interesting insulation properties: heat transmission ranges from 0.06 to 0.19 Wm-1K-1 for dry apparent densities between 200 and 840 kg/m3 [Bütschi 04, Cérézo 05, Nguyen 09]. Nevertheless, the compressive strength of this material is less than 2 MPa [Bütschi 04, Eires 06, Elfordy 08, Bruijn 09, Arnaud 11, Kioy 05]. This low compressive strength, in combination with the low Young's modulus of the LHC mixtures (cf. Tab.1), indicates that the material in its present form cannot be used as a load-bearing material. More rigidity and higher compressive strength are needed.

LHC walls can be made on site, the material poured in a framework and tamped manually, or sprayed using a projection process. These processes do neither achieve a high compactness or any precise control of conditions of maturation of the material. As a consequence, its resistance is very low. For example, French professional LHC building rules [CenC 12] give a compressive strength of 0.3 MPa for tamped LHC walls and floors. LHC can also be used to make bricks, or hollow blocks. The main asset of this method is to permit a better control of packing and arrangement of particles. This is the process developed in the present work.

Two main ways are studied to improve the strength of hollow blocks made of plant-derived aggregates and cementitious binders. The first one is the use of an admixture. For example, Nozahic and Amziane [Nozahic 12a] have treated the surface of sunflower aggregates to improve fiber-matrix bonds. Kazhma et al. [Kazhma 08] have used sucrose to treat flax shiv by cement–sucrose coating. This gives promising results, but requires an additional stage of processing and additives to be achieved. The second way to improve the material properties is a controlled compaction of the fresh mixture during moulding. Nguyen et al. [Nguyen 09a, Nguyen 09b, Nguyen 10] have shown that the compaction of fresh material can increase significantly the compressive strength of hemp concrete by reducing the volume of voids within the material. Such a process improves mechanical strength while using lower binder contents. It also magnifies the strain capacity before collapse. Compacted LHC is pressed during casting. The aim is to have a structural or load-bearing function, while keeping good thermal insulation properties. Fig. 1 draws typical curves of uniaxial compressions on LHC cylinders found in literature. It clearly shows the improvement due to the compaction process on both rigidity and ductility. For compacted LHC blocks,

extracting a value of yield stress or strength is not as easy as for classical building materials, which pass by a maximum value, corresponding to the compressive strength [Arnaud 00, Cérézo 05, Kioy 05]. Nguyen et al.[Nguyen 09a] choose arbitrary values for compacted blocks: stresses for a strain of 1.5%, close to the end of the linear elastic area and 7.5% in the strain hardening area. Tab.1 gives the principal results for strength deduced from literature and computed with these arbitrary characteristics.

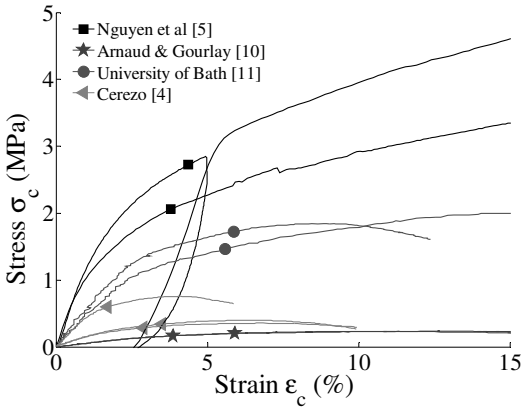

Fig.1 The different compressive curves of LHC found in literature: low compactness LHC [10; 4; 11] behave as light concretes, with a stress softening and densest LHC [5] have a large hardening area.

However the pressure applied by the upper punch of the compression cell by Nguyen et al. and in former studies was never higher than 2.5MPa. This upper limit is due to the design of the compression cell (generally made of polymeric materials as PVC). Higher compressive stresses are required to limit the proportion of binder, which is the main environmental impacting component of LHC, and to improve the hollow block's resistance and rigidity. Nozahic et al. [Nozahic 12b] made prismatic 40x40x160mm3 specimens by applying a upper pressure of 5MPa on bio-aggregates, pumice and lime mixtures. But the binder/aggregate mass ratio was 18, and the specimens are narrow compared with the size of the longest particles (40mm). That's why Tronet et al. [Tronet 14] developed a steel cylindrical rigid die, applying upper pressures on fresh mixtures up to 10 MPa and making 10cm-in-diameter and 20cm-in-height specimens. They show that high level of compression can be a good way of limiting heterogeneity inside the precast block, and that for high levels of compression mix design doesn't really influences the heterogeneity of loading. In the present paper, the same device as [Tronet 14] is used to produce cylinder blocks from several mixtures. Their compressive behaviour is then studied at the age of 28 days.

In literature, the strength of hardened LHC is essentially caused by the properties and proportion of the binder chosen for its formulation. Lanos et al. [Lanos 13] recall that the mechanical results for mineral binders can be modeled by a power law based on the volume fraction ϕ occupied by the hardened binder in the sample of hardened paste:

$$\sigma = \sigma_0 . \phi^a \quad (1)$$

where σ_0, obtained for $\phi = 1$, is the intrinsic strength of the binder without any porosity. Nguyen et al.[Nguyen 09a] found a σ_0 of 126,2 MPa by studying the effect of W/B on lime paste resistance (studied lime was Tradical ® PF 70). The parameter *a* usually takes a value of around 2 for cementitious materials. Nguyen et al. give a value of 2.98 for the Tradical ® PF 70 and Nozahic et al.[Nozahic 12b] take a value of 3 with a pumice- lime binder.

For hardened mixes with hemp shiv, this law of variation of the binder's strength could be adjusted, considering that the inert load corresponding to the hemp shiv plays no part in the strength of the mixture, other than by the effect of dilution. The strength of the mixture could then be given by:

$$\sigma = \sigma_0 . (\phi . V)^a \quad (2)$$

where V is the volume proportion of hardened paste (of solid volume fraction ϕ) in a cubic meter of LHC. This type of law is quite in accordance with the trends indicated by works on sprayed and tamped LHC [Cérézo 05, Elfordy 08, Bruijn 09, Arnaud 11, Kioy 05], or on very rich-in-binder compacted mixes [Nozahic 12b]. But in the case of highly compacted blocks [Nguyen 9a], equation 2 doesn't fit the experimental results. The compaction of the fresh mix induces other mechanics that improve the strength. In this case, shiv should play a part. Its particles compactness will be higher than in natural (bulk) conditions. Actually, the fresh mixture undergoes a pressure to be compacted, and should be able to undergo a same order of pressure at hardened state before yielding or collapsing.

Tab. 1. Some strength and stiffness of LHC deduced from literature (W/B= Water to binder mass ratio ; B/S= Binder to shiv mass ratio).

	W/B	B/S	**Density** *(hardened state)* **[kg/m3]**	$\sigma_{1,5\%}$ [MPa]	$\sigma_{7,5\%}$ [MPa]	E [Mpa]
Nguyen [5]	0,55	2.15	850	1.58	3.57	131
	0,86	2.15	670	1.34	2.65	113
Arnaud & Gourlay [10]	1,5	2.4	460	0.08	0.22	5
Kioy [11]	1,1	1.9	610	0.70	1.65	43
	0,8	1.9	830	0.86	1.82	52
Cerezo [4]	1,3	8	356	0.21	0.35	14
	1,3	6.7	391	0.22	0.39	44
	1,4	5.3	504	0.57	-	15

The main objectives of this paper are 1/To show the potential and the limitations of casting LHC hollow blocks at high level of compression; 2/To demonstrate that compressive strength can be improved when lime is replaced by shiv in mix design; 3/ to adapt the current strength formula (Eq2) to fit with compressed LHC.

2 CASTING OF LHC BLOCKS: MATERIAL AND PROTOCOL

2.1 Material

Aggregates

In this study, the shiv has been totally separated from fibers using a mechanical grinding process. This

aggregate is characterized by a very low bulk density (about 110 kg/m3) because of its highly porous structure. The size of capillaries ranges from 10 to 50 µm inside aggregates. As a consequence, this aggregate exhibits a high water absorption capacity: up to 320% of its own mass, after 48h immersion, and 270% after a few minutes [Nguyen 09a; Chamoin 11]. The specific density of this shiv (cell walls of particles without internal porosity) has been measured in a picnometer: it is about 1465 kg/m3. Particle density of shiv is 280kg/m3 measured by Pham [Pham 14]

Binder

A lime based binder called Tradical ® PF 70 (Lhoist group) was used. It consists of 75% hydrated lime Ca(OH)2, 15% hydraulic lime, and 10% pozzolana. Its specific density, given by the supplier, is 2450 kg/m3.

2.2 Mix designs and compression process at fresh state

Based on Nguyen et al. [Nguyen 09a, 09b], five LHC mixes were designed to explore the suitability of mixtures with a high shiv proportion, by applying high pressures in a cylindrical matrix. The capillary and deformable character of shiv makes mixing more difficult than for traditional concrete or mortar. The mixing phase consists in two steps: 1/mixing of shiv and water during 4 minutes at 140 rpm in a planetary Hobart mixer; 2/ adding lime and mixing during 4 minutes at 140 rpm. During the first step, the water is totally absorbed by the shiv. This means that the second step is similar to the mixing of dry particles. Water is released by aggregates as they are pressed in the compression cell. The amount of water needs to be calculated as a function of binder content, considering that most of water becomes available for lime wetting and hydration at the end of compaction. The mixtures are presented on Tab.2. W/B is the Water to Binder mass ratio, equal to 0.55 for each LHC mixture. B/S is the Binder to Shiv mass ratio. The compression device is composed of a steel 100mm-inner-diameter cylinder, a fixed lower punch, and a moving upper punch. The piston rod of the upper punch is screwed under a 250kN press, equipped with force and displacement transducers. The thickness of the cylinder wall is 10mm, ensuring a negligible strain up to a radial pressure of 10MPa**.** This compression device is more precisely described in [Tronet 14].

The mean upper pressure σ_{zUP} can be deduced from the force transducer measurement F_{UP} of the press:

$$\sigma_{zUP} = F_{UP}/\pi R^2 \quad (3)$$

where R is the inner radius of the compression die (Fig. 2). Maximum upper stresses reached at the end of compaction step are given on Tab. 2.

The initial (bulk) apparent volume of the mixture poured into the cylinder is three to four times the final compacted apparent volume. The target value for the final height was 200mm for every specimen. Every test is controlled in displacement, with the same upper punch speed of 1mm/s.

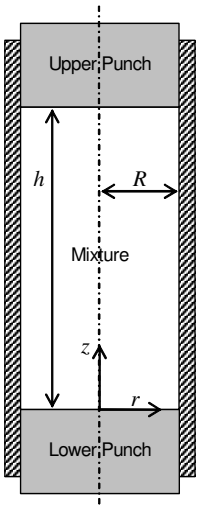

Fig.2 Bench mark and geometry of the compression device

At the end of compression step, the specimen reaches a given compactness, called “green compactness” in Tab. 2. Compactness is effectively the most significant parameter to characterise the compaction state, due to the difference of specific gravity between water, shiv and lime. At fresh state, compactness corresponds to the sum of solid volume fraction and liquid volume fraction, i.e. the volume of liquid and solid divided by the total volume of the sample. The liquid phase is included because it is assumed to be physically linked to lime and shiv at the end of compression step. This assumption is valid as soon as the water content is low, ensuring that no free and draining water exits from the sample. And effectively during compression, no loss of mass was recorded. At the end of compression process, each specimen is maintained in compression, keeping a height of 200 mm, during 72 hours. This step is needed to ensure a minimum hydration of lime, avoiding capping and elastic release of the specimen when pushing out of the die. LHC blocks are then placed in a room controlled in temperature (20±1°C) and humidity (70±5%), until the age of 28 days. Some of this LHC blocks (M4 and M5) must also be clamped during maturation to avoid visco-elastic release. During ageing of LHC specimens, some liquid water is consumed by lime hydration and a large amount is evaporated. Then the compactness of samples decreases, as seen in Tab. 2.And this compactness decreases much more when paste contents are high. Samples are finally tested by uni-axial compression, at 28 days.

2.3 Simple compression at hardened state: typical curves and characteristic parameters

At least five specimens where processed for each LHC mixture (M1 to M5). After three days of hydration and relaxation in the compression cell and 25 other days in air-conditioned room, a simple compression test was done on each specimen. These tests were cyclic, to observe elastic parameters evolution with strain, and to evaluate the damage or hardening of the samples. These measures won’t be developed in the present paper. The compressions are controlled in displacement under a press fitted with axial force and displacement transducers.

Tab 2. Studied mixtures

	Shiv (S) [kg] (In a	Binder (B) [kg] m^3 of	Water (W) [kg] LHC)	W/B	B/S	Upper compression Stress [MPa]	Green density (kg/m3)	Green compactness [-]	Compactness after 28 days of ageing [-]
M1	215	387	213	0.55	1.8	1.1	816	0.52	0.37
M2	257	360	198		1.4	1.7		0.52	0.39
M3	320	320	176		1	2.6		0.53	0.4
M4	500	270	148		0.54	6.7	920	0.6	0.55
M5		204	112		0.41	6.3	816	0.54	0.5

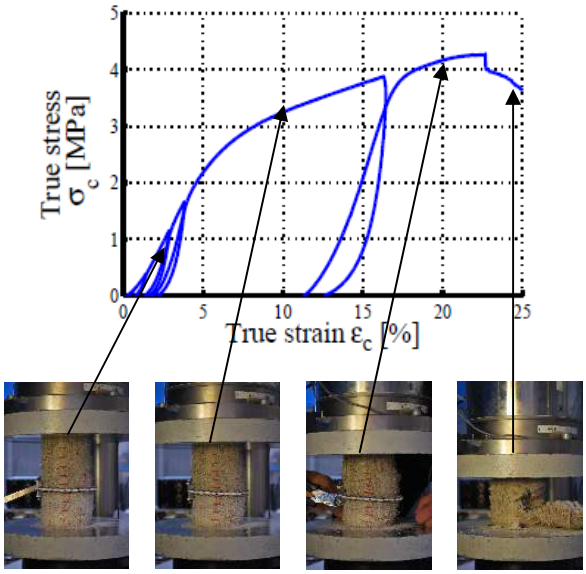

Fig. 3: Typical compression curve for strength and characterisation of hardened LHC

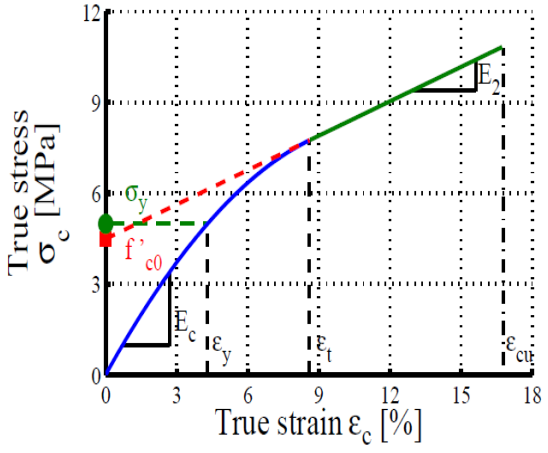

Fig. 4: Parameters of Lam&Teng.

Fig. 3 shows the typical force-displacement curve for a compressed LHC block. Contrary to conventional building materials, LHC compressed blocks behave as foam with a small "purely elastic" range and a large "plastic" range. The plastic range can itself be divided in two zones:

- A first zone corresponds to the closing of the voids, firstly between shiv particles and secondly inside the particles themselves. Both result in a quasi linear strain hardening.

- A second zone where voids are almost closed, making the granular packing more rigid.

In this study, only elastic and linear hardening ranges will be considered. Taking into account the large deformations of this material, the true strain is used for stress-strain curves: $\varepsilon_c=\ln(h/h0)$.

The strength parameters given in Tab.1 are arbitrary parameters. In this study, more objective parameters are proposed to characterize stress-strain behaviour of the composite. Lam and Teng [Lam 09] proposed a model to fit FRP-confined concretes experimental curves. These curves have the same shape as compression of LHC blocks up to the end of linear hardening stage. Their model consists of firstly a parabolic zone and a linear second zone with a smooth transition at a strain ε_t.

The monotonic curve envelope is defined by the two following relationships (Fig.4):

1. for the elastic zone ($0 \le \varepsilon_c \le \varepsilon_t$):

$$\sigma_c = E_c\ \varepsilon_c - \varepsilon_c^2\ (E_c-E_2)\ /(4\ f'_{c0}) \quad (4)$$

2. for the strain-hardening zone ($\varepsilon_t \le \varepsilon_c \le \varepsilon_{cu}$):

$$\sigma_c = f'_{c0}+E_2\ \varepsilon_c \quad (5)$$

Where σ_c is the compression stress; ε_c is the true compression strain; ε_{cu} is the maximum strain used to fit the curve; Ec is the apparent elastic modulus; f'c0 is considered to be the apparent compression strength given by the intercept point of Y-axis and the extent of the linear hardening line; E2 is an apparent hardening modulus, corresponding to the slope of the linear hardening part. ε_t is the strain at which hardening begins. This strain can then be computed as follows:

$$\varepsilon_t = 2\ f'_{c0}/(Ec-E2) \quad (6)$$

This means that the extended linear hardening line (slope E2) intersects the extended linear elastic line (slope Ec) at a compressive strain $\varepsilon_c=\varepsilon_t/2$.

In the following development, this strain will be considered to be the strain at which irreversible deformations begin. The yield stress σ_y can then be computed as the stress at $\varepsilon_t/2$:

$$\sigma_y = \sigma_c\ (\varepsilon_t/2) = \sigma_c\ (f'_{c0}/(E_c-E_2)) \quad (7)$$

The characteristics of the mix designs from Tab.1 and Fig.1 have been computed by means of this model. The parameters obtained by this mean are given in Tab.3.

3 RESULTS

Fig.5 shows the curves of simple compression tests on mixes M1 to M5. Tab. 5 also gives the values computed from these curves using the method described in section 2. For similar green compactness (M1, M2 and M3), apparent elastic modulus and strength slightly increase with binder to shiv ratio.

However an increase of 80% in binder content only leads to a gain of 20% in strength. On the contrary, when a lower proportion of binder is counterbalanced by a higher compactness (for example comparing M3 and M5), rigidity and compressive strength are improved.
to a difference of water content. Furthermore, for mixes M1 to M5, with the same water to binder ratio, σ_y appears to decrease with B/S for M1 to M3, and to drastically increase with B/S between M3 and M5.

Tab. 3 Compressive yield strengths,deduced of Lam and Teng Model

	W/B	B/S	Density *(hardened state)* [kg/m3]	σ_y [MPa]
Nguyen 09a	0,55	2.15	850	2
	0.86	2.15	670	1.4
Arnaud 11	1.5	2.4	460	0.2
Kioy 05	1.1	1.9	610	1.1
	0.8	1.9	830	1.2
Cerezo 05	1.3	8	356	0.2
	1.3	6.7	391	0.5
	1.4	5.3	504	0.2
M1	0.55	1.8	580	1.4
M2	0.55	1.4	612	1.6
M3	0.55	1	616	2.1
M4	0.55	0.54	843	4.7
M5	0.55	0.41	756	4

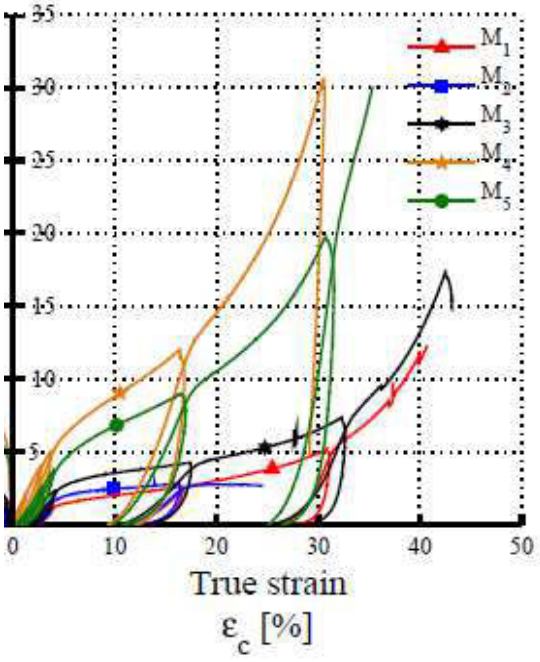

Fig. 5: Axial stress-strain behaviour of the five mix design

It is widely accepted that a key parameter in mechanics of building materials is porosity (i.e. the compactness). In the present case the porosity in the hardened state is controlled by two factors in the fresh mix: the quantity of water and the compactness

3.1 Behaviour at the age of 28 days

Comparing values of B/S, σ_y and Ec in Tab.3, it is apparent that B/S is not the only key parameter. For example, one can compare the two mixes of Nguyen et al.: B/S=2.15 for both the mixes and σ_y is different, due

achieved. With an excess of water in the fresh mix (case of [Arnaud 11], [Kioy 05] and [Cérézo 05]), most of the water will be lost from the composite during drying and hardening and the hardened LHC will be more porous. Comparing M1 and M3, which have the same order of compactness in the hardened state, the binder content has a slightly positive effect on strength and rigidity. On the contrary, when B/S is reduced by a factor in excess of two (1.00 for M3 and 0.41 for M5) and the compactness is high, due to the level of compression in casting, the strength and rigidity are largely improved.

These results imply that the main controlling factor governing the strength of a compressed LHC block appears to be the compactness in the hardened state, that is to say controlled by the compressive stress during casting in the fresh state.

A number of the results in Tab.3 are used to determine the relationship between yield stress and compactness at 28 days of maturation, Fig.6.

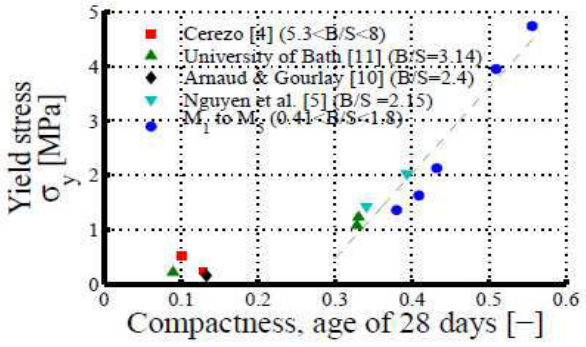

Fig. 6: Yield Stress versus Compactness at 28 days of maturation from published mix designs and M1 to M5

With regard to the yield stress, Fig.6 shows there is an almost linear relationship with compactness above a given threshold of compactness. This threshold of compactness appears to be of the order of 0.25 and it corresponds to a compactness at which shiv and lime particles percolate and have completed their rearrangement. Above this limit, the hardening of binder paste is not the only factor that controls the compressive strength of the material. Shiv particles undergo intrinsic deformation in the fresh state that result in creep effects in the hardened state. The compaction mechanisms can be distinguished in three steps, as first described by Seeling and Wülff [Seeling 46]:

1. Packing of particles, attainable with a low level of pressure, up to a rearrangement compactness Cr;

2. Elastic and plastic deformation of particles to fill inter-particles porosities and to reduce intra-particles porosities under a higher pressure;

3. Fragmentation (in the case of brittle particles).

In the fresh state, if the mix is not compacted, the maximum compactness of binder paste C_{pmax} corresponds to the inter-particles porosity:

$$C_{pmax}=1-S/\rho_{particles}=B_{max}/\rho_B + W_{max}/\rho_W \qquad (8)$$

[Lanos 13] found that in the presence of non-fibrous hemp shiv and classical hydrated lime, the ratio W/B

by mass of the binder paste should be about 0.56, any excess water being entrapped in capillaries of shiv particles. In the case of M1 to M5, the initial W/B ratio is 0.55 that is very close to the value suggested by Lanos et al.

It is possible to compute the maximum compactness of hardened LHC without causing compression inside the shiv particles:

$$C_{max}=C_{pmax}+S/\rho_S-(W/B)\ B_{max}/\rho_W+(t-1).B_{max}/\rho_W$$

$$=1-S.[1/\rho_{particles}-1/\rho_S+(B/S)_{max}.(1-t+W/B)/\rho_W)] \quad (9)$$

Where

• S is the shiv content [kg in a m3 of LHC mix];

• Bmax is the maximum binder content without compression, Bmax= Cpmax /(1/ ρB +(W/B)/ρW);

• ρ_W , ρ_B, and ρ_S are respectively the density of water, the specific density of the binder, and the specific density of the shiv;

• W/B is equal to 0.55 or 0.56

• $\rho_{particles}$ is the particle apparent density of the shiv, found to be 280kg/m3 in [Pham 14]

• t is the hydration degree, known to be 1 for an aerated lime and 1.25 for a Portland cement. Here we consider the hardened state at about 28 days, with negligible carbonation. Tradical PF70 contains 25% in mass of cementitious materials, and a value of 1.1 was chosen for t.

With the densities given in section 2 for the materials, and a degree of hydration of 1.1, the maximum of compactness without reduction in the volume of shiv particles ranges between 0.177 (B/S=0) and 0.378 (B/S=5.42). B/S =5.42 corresponds to the ratio above which density of the shiv packing, in a non compressed configuration, is less than bulk density inside LHC. Above this limit, the binder volume is too high to permit a proper shiv percolation. Therefore binder behaviour will be the dominant mechanism from a mechanical point of view.

4 A PREDICTIVE MODEL FOR LIME-HEMP CONCRETES

4.1 Correlation between yield strength, compaction and binder content

Based on the observations made in the previous sections, a model is proposed to predict the strength of LHC as a function of mix design and casting process. The mix design takes into account a compactness state that results in a reduction of the shiv particles. This compaction state can be achieved manually up to the rearrangement compactness; if this is not achievable manually a press will be needed. Tronet et al. [Tronet 14] have applied several compaction models to mixes in the fresh state; these included complete mixes and dry mixes. A dry mix being one in which water has been eliminated from the mix constituents. It has been shown that the presence of water softens the shiv particles. Mixes without water are more difficult to compact than complete mixes.

Jones [Jones 60] proposed a simple model (Eq11) to relate compactness and stress.

$$C=(\sigma_{zUP}/\sigma_1)^{1/b} \quad (11)$$

Where C is the compactness, σ_{zUP} is the upper stress applied during compression and '1/b' is a constant called 'compressibility'. In a compression cell in the fresh state, compressibility ranges between 0.27 and 0.4 for complete mixes M1 to M5 and between 0.14 and 0.27 for dry mixes M3 to M5 [Tronet 14]. In the case of hardened LHC, this compressibility should approximately correspond to those of dry mixes (1/b ≈ 0.2, and then b ≈ 5). σ_1 corresponds to the stress that should be reached to attain a dense packing of the material, corresponding to a compactness C = 1. σ_1 can be computed from the compression results on dry mixes. For dry shiv alone it gives a value of 233MPa [Tronet 14].

In an attempt to quantify the component of the stress that is taken by the shiv skeleton, Eq11 can be adapted as follows:

$$\phi_S/\phi_{Smax}=S/S_{max}=(\sigma/\sigma_s)^{1/b} \quad (12)$$

With σ_S the theoretical stress needed to obtain dense particles of shiv in the packing, ϕ_S the solid volume fraction of shiv in LHC. S_{max} is the mass of shiv in a cubic metre of hardened LHC which is correlated to the maximum solid volume fraction ϕ_{Smax}. The value of ϕ_{Smax} is that that could theoretically be achieved by the shiv packing in hardened LHC if the stress σ_S could be reached. Considering that hydrates and binder particles are incompressible the following relationship can be developed:

$$C=1=\phi_{Smax}+B/\rho_B+B(t-1)/\rho_W=S_{max}/\rho_S+B[1/\rho_B+(t-1)/\rho_W] \quad (13)$$

S_{max} could theoretically be reach by reduction in volume of the LHC. During a compression test the B/S ratio remains constant, therefore S_{max} can be expressed as a function of B/S:

$$S_{max}=1/[1/\rho_S+B/S\ [1/\rho_B+(t-1)/\rho_W] \quad (14)$$

It follows that taking into account the effect of paste hardening (Eq.2) and load bearing by the shiv skeleton (Eq.12), a formula for the prediction of the yield stress in the hardened state can be proposed:

$$\sigma_y=\sigma_B\ (\phi_B)^a+\sigma_S\ (\phi_S/\phi_{Smax})^b \quad (15)$$

Where σ_B is the specific strength of the lime, ϕ_B the volume solid fraction of binder in the hardened LHC, *a* is a constant computed from uniaxial compression tests on binder pastes with different W/B ratios, which are close to 2 for cement and 3 for lime [Nguyen 9a, Nozahic 12b].

Considering B and S, the binder and shiv masses in a cubic metre of LHC, Equation 15 can be written for the 28 days age:

$$\sigma_y=\sigma_B\cdot\left(B\cdot\left(\frac{1}{\rho_B}+\frac{t-1}{\rho_W}\right)\right)^a+\sigma_S\cdot\left(S\cdot\left[\frac{1}{\rho_S}+(B/S)\cdot\left(\frac{1}{\rho_B}+\frac{t-1}{\rho_W}\right)\right]\right)^b \quad (16)$$

With ρ_B=2450kg/m^3, ρ_W=1000kg/m^3, ρ_S=1465kg/m^3, σ_B=126.2MPa and a=2.98 [Nguyen 09a], σ_S=233MPa [Tronet 14], t=1.1. *b* is the only fitting parameter; a value of 5.1 provides a good agreement with the tests in this study. A value of the order of 5 is in agreement with those reported in [Tronet 14]. Eq16 is valid when the shiv percolation is sufficient to bear the load, which corresponds to $S>S_{bulk}$=110kg/m^3, and B/S<5.42. If this is not the case, only the first term of (Eq16) must be used.

Eq16 enables strength prediction and the selection of shiv binder proportions for a required yield stress. It is

possible to draw the iso-strength lines from Eq16 in a B-S plane, as shown in Fig.7. As noted in the introduction, the degree of compaction of LHC is dependent on the method of placement: compression due to spraying or tamping, compression in a press for manufactured blocks or no compression for roof applications. [Lanos 13] introduced a compacting coefficient for shiv which expresses the reduction in volume accessible to the paste. This compacting coefficient c_c is expressed as:

$$c_c = \rho/\rho_{bulk} \quad (17)$$

where ρ_{bulk} is the apparent density of the hemp shiv packing without compression and ρ is the apparent density of the hemp shiv packing in its compacted state achieved by a particular placement method. [Nguyen 09a] showed that attaining a compacting coefficient of 1.5 requires quite a low level of pressure, but that a compacting coefficient above 2 is unattainable with traditional placing techniques. The compacting coefficient of shiv, to reach the compactness corresponding to the particle density, is c_c =280/110=2.54. This can be considered to be the compacting coefficient for which the rearrangement of shiv particles is without doubt achieved. In fact, from a process point of view, binder particles and water fill the packing and change both the bulk compactness and the rearrangement compactness. These parameters have been measured in [Tronet 14] for fresh mixes M1 to M5. The results show a linear trend of compactness with B/S ratio: bulk compactness C_0=0.13+0.025 B/S and rearrangement compactness C_r=0.29+0.032 B/S. It is then possible to estimate the compacting coefficient of the mixes corresponding to the end of rearrangement phase: $c_{LHC}= C_r/C_0$. By this method, the value of c_{LHC} was found to range from 1.74 for B/S=5.42 to 2.16 for B/S=0.4. The compacting pressure increases rapidly above C_r. These c_{LHC} values can be used as a limit between a manual process and the necessity to use a press; this limit is drawn on Fig 15. It is valid for W/B=0.55 and should be adapted for other W/B. One can remark that C_0 = 0.13, for a B/S=0, is a little higher than the compactness related to the bulk density of shiv alone (ρ_{bulk}=110kg/m^3 => C0=0.08). This difference is due to the presence of water that fills the packing and facilitates rearrangement.

Choosing B and S masses in a cubic metre of mix will correspond to a given compacting coefficient of the mix in the fresh state. The compaction coefficient of the mix c_{LHC} can be computed as follows:

$$c_{LHC} = C_{\text{fresh state, compacted}}/ C_0 = (S/\rho_S+B/\rho_B+W/\rho_W)/ C_0$$

$$c_{LHC} = S.[1/\rho_S+B/S(1/\rho_B+W/B.\ 1/\rho_W)]/(0.13+0.025\ B/S) \quad (18)$$

The iso-compaction lines can then be computed, and drawn on Fig 7.

This diagram gives some indications about formulating the material design and behaviour: without compaction, yield stress will hardly reach 0.5 MPa unless an excessive amount of binder is used ; with a manual compaction pressure, a diminution of B/S will rapidly decrease the strength in the hardened state ; for the same compaction state, increasing binder proportion will always improve the strength ; for the same binder to shiv ratio by mass, the compaction state is the dominant factor for achieving strength ; to reach a strength of 10 MPa requires a really high binder content (up to 700 kg/m^3), or a high level of compaction (compacting coefficient up to 4.5).

5 CONCLUSION

A compression device was designed to explore factors controlling stiffness and strength of lime-hemp composites. The experimental results, augmented with some results taken from literature, help to develop an understanding of this material:

• To reach levels of strength in the hardened state comparable to those of concrete or clay bricks, a press must be used to achieve the required level of compaction.

• Compaction of a block is a good mean to improve strength when increasing the shiv proportion.

• Shiv will contribute to strength when the volume of particles is reduced during the casting process. This reduction in volume of particles starts with a rearrangement compactness that corresponds to a volume reduction of about 2.

• The stiffness also depends on compactness, but will be reduced by a high shiv content because walls of the shiv particle are one order more flexible than binder particles.

A model has been proposed to predict the strength from the mix composition and the compacting state during casting. It allows the mix design of an LHC composite and gives an indication as to the type of compaction required during fabrication

6 REFERENCES

[Arnaud 00] Arnaud L, Mechanical and thermal properties of hemp mortars and wools: experimental and theoretical approaches, Bioresources Hemp 2000

[Arnaud 11]Arnaud L, Gourlay E. Experimental study of parameters influencing mechanical properties of hemp concrete, Construction and building materials 2011;28:50-56.

[Boutin 06] Boutin MP, Flamin C, Quinton S, Gosse G. Etude des caractéristiques environnementales du chanvre par l'analyse de son cycle de vie. Ministère de l'agriculture et de la pêche, France, 2006.

[Bruijn 09] Bruijn PB, Jeppsson KH, Sandin K, Nilsson C. Mechanical properties of lime – hemp concrete containing shives and fibres. Biosystems Eng 2009; 103: 474-479.

[Bütschi 04] Bütschi PY. Utilisation du chanvre pour la préfabrication d'éléments de construction. PhD Thesis, Moncton University, Moncton, Canada, 2004.

[CenC 12] Construire en chanvre, règles professionnelles d'exécution de construction, SEBTP 2012, ISBN : 978-2-35917-046- 7

[Cérézo 05] Cérézo V. Propriétés mécaniques, thermiques et acoustiques d'un matériau à base de particules végétales : approche expérimental et modélisation théorique. PhD Thesis, INSA Lyon, France, 2005.

[Chamoin 11] Chamoin J, Collet F, Pretot S, Lanos C. Réduction du pouvoir absorbant de chènevottes par traitement imperméabilisant, Matériaux & Techniques 2011, EDP Sciences, 99(6), 633–641.

[Eires 06] Eires R, Nunes P, Fangueiro R, Jalali S, Cameos A. New eco-friendly hybrid composite

materials for Civil construction. European Conference on Composite Materials. Biarritz, May, 2006.

[Elfordy 08] Elfordy S, Lucas F, Tancret F, Scudeller Y, Goudet L. Mechanical and thermal properties of lime and hemp concrete (« hempcrete ») manufactured by a projection process. Construction and Building Materials 2008;22 (10):2116-2123.

[Jones 60] Jones WD. Fundamental principle of powder metallurgy, Edward Arnold Publisher Ltd, London, UK, 1960

[Khazma 08] Khazma M, El Hajj N, Goullieux A, Dheilly RM, Queneudec M. Influence of sucrose addition on the performance of a lignocellulosic composite with a cementious matrix. Composites: Part A 2008;39:1901-1908.

[Kioy 05] Kioy S. Lime-hemp composites: compressive strength and résistance to fungal attacks. MEng dissertation, University of Bath, 2005, recalled in Appendix 1: Resistance to compression and stress-strain properties, In: Bevan Rand Woolley T, editors. Hemp Lime Construction, A guide to building with hemp lime composites, IHS BRE press, 2013. p. 101-104

[Lam 09] Lam L, Teng JG. Stress–strain model for FRP-confined concrete under cyclic axial compression. Engineering Structures, 2009,31(2): 308–321.

[Lanos 13] Lanos C , Collet, F, Lenain G, and Hustache Y. Formulation and implementation, In: Amziane S, Arnaud L, editors. Bio-aggregate-based Building Materials. London/Hoboken: ISTE/Wiley, 2013 : 117-152.

[Nguyen 09a] Nguyen TT, Picandet V, Carré P, Lecompte T, Amziane S, Baley C. Effect of compaction on mechanical and thermal properties of hemp concrete, EJECE 2009;13:1039-1050.

[Nguyen 09b] Nguyen TT, Picandet V, Amziane S, Baley C. Influence of compactness and hemp hurd characteristics on the mechanical properties of lime and hemp concrete, EJECE 2009;13:1039-1050. [Nguyen 10] Nguyen TT. Contribution à l'étude de la formulation et du procédé de fabrication d'éléments de construction en béton de chanvre, PhD thesis, Université de Bretagne-Sud, 2010.

[Nozahic 12a] Nozahic V, Amziane S. Influence of sunflower aggregates surface treatments on physical properties and adhesion with a mineral binder, Composites: Part A 2012;43:1837-1849

[Nozahic 12b] Nozahic V, Amziane S, Torrent G, Saïdi K, De Baynast H. Design of green concrete made of plant-derived aggregates and a pumice-lime binder Cement and concrete composites 2012, 34, 231-241..

[Pham 14] Pham T.H., Modélisation multi-échelles des propriétés thermiques et élastiques de composites chaux-chanvre, PhD thesis, Université de Bretagne-Sud, 2014.

[Picandet 13] Picandet V. Characterization of Plant-Based Aggregates. In: Amziane S, Arnaud L, editors. Bio-aggregate-based Building Materials. London/Hoboken: ISTE/Wiley, 2013:27-73.

[Seeling 46] Seeling P, Wulff J. Pressing operation in fabrication of articles by powder metallurgy, Trans. Am. Inst. Mining. Met. Engrs, 1946; 166: 492-505

[Tronet 14] Tronet P, Lecompte T, Picandet V, Baley C. Study of lime and Hemp composite precasting by compaction of fresh mix – A Fitted die to measure friction and stress state, Powder Tech., 2014, 258:285-296.

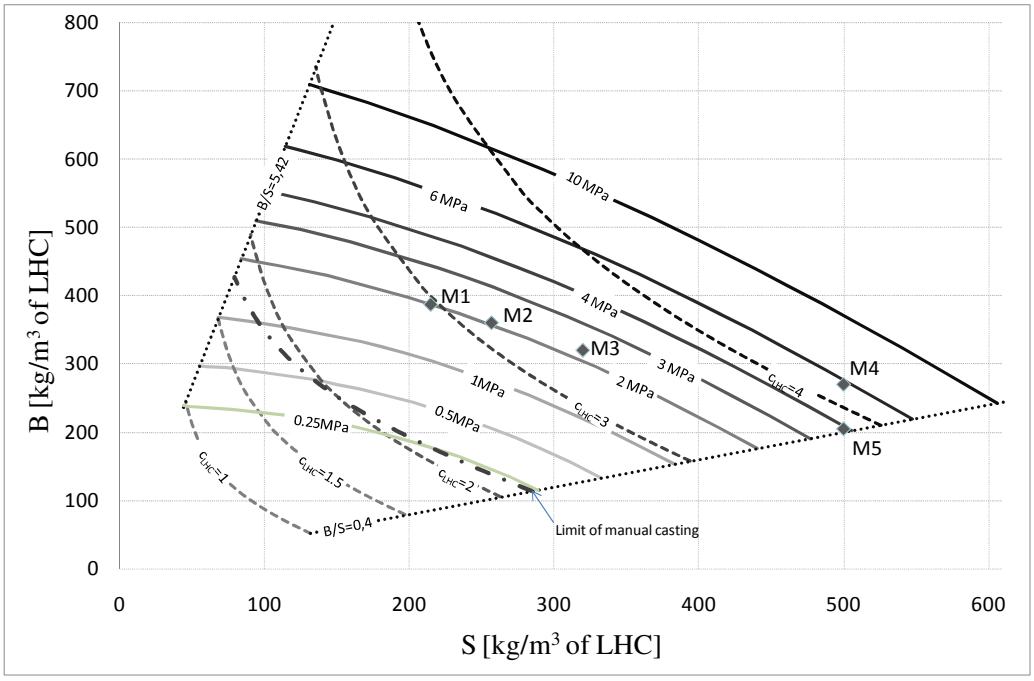

Fig. 7. Design chart for selecting B and S, and the consequence of B and S content on the process compacting coefficient (cLHC). Curves are drawn for W/B=0.55, Binder Tradical PF 70 (hydration degree t=1.1), Hemp Shiv of specific density 1465 kg/m3, particle density 260 kg/m3 and bulk density 110 kg/m3